

Supporting Information

Promoting the Sulfur Immobilization by a Hierarchical Morphology of Hollow Carbon Nanospheres Cluster for High-stability Li-S Battery

Mingqi Chen^a, Zhe Su^a, Kai Jiang^a, Yankai Pan^a, Yayun Zhang^{*a}, Donghui Long^{*a,b}

^a State Key Laboratory of Chemical Engineering, East China University of Science and Technology, Shanghai 200237, China

^b Shanghai Key Laboratory of Multiphase Materials Chemical Engineering, East China University of Science and Technology, Shanghai 200237, China

* Corresponding author:

Tel: +86 21 64252924. Fax: +86 21 64252914.

E-mail: longdh@mail.ecust.edu.cn. (Donghui Long); yy.zhang@ecust.edu.cn.(Yayun Zhang).

Figures and Tables:

Figure S1. SEM image of HCNCs.

Figure S2. TEM images of HCNCs obtained with different RF precursor concentration.

Figure S3. TGA curves of pomegranate-like SiO₂/C clusters and single SiO₂/C nanosphere under air atmosphere.

Figure S4. X-ray photoelectron spectroscopy (XPS) analysis of HCNCs-1.

Figure S5. TGA curves of MHCSs and HCNCs under air atmosphere.

Figure S6. Raman spectra of HCNCs and MHCSs.

Figure S7. XRD patterns of MHCSs and HCNCs.

Figure S8. (a-d) SEM images of MHCSs, MHCSs/S, HCNCs-1 and HCNCs-1/S, respectively.

Figure S9. High-resolution S 2p spectra of HCNCs-2/S.

Figure S10. Nyquist plots of MHCSs/S and HCNCs/S before cycling and after 100 cycles at 0.5 C rate.

Figure S11. SEM image of the fresh (a, c) and cycled (b, d) electrodes in a charge state after 200 cycles at 1 C. Insets of (a-d) are corresponding local magnification SEM images.

Figure S12. (a) Cycle performance of HCNCs/S and MHCSs/S electrodes with a high-sulfur-loading of 4 mg cm⁻² at 0.2 C. (b) Rate performance of HCNCs-2/S electrode with a high-sulfur-loading of 4 mg cm⁻² at varied current rates.

Table S1. XPS results of MHCSs/S and HCNCs/S.

Table S2. Elemental analysis of MHCSs/S and HCNCs/S.

Table S3. Electrode resistance obtained from equivalent circuit fitting of the HCNCs/S and MHCSs/S cathode.

Table S4. Electrochemical performances comparison of HCNCs/S with the reported hollow carbon/sulfur cathodes.

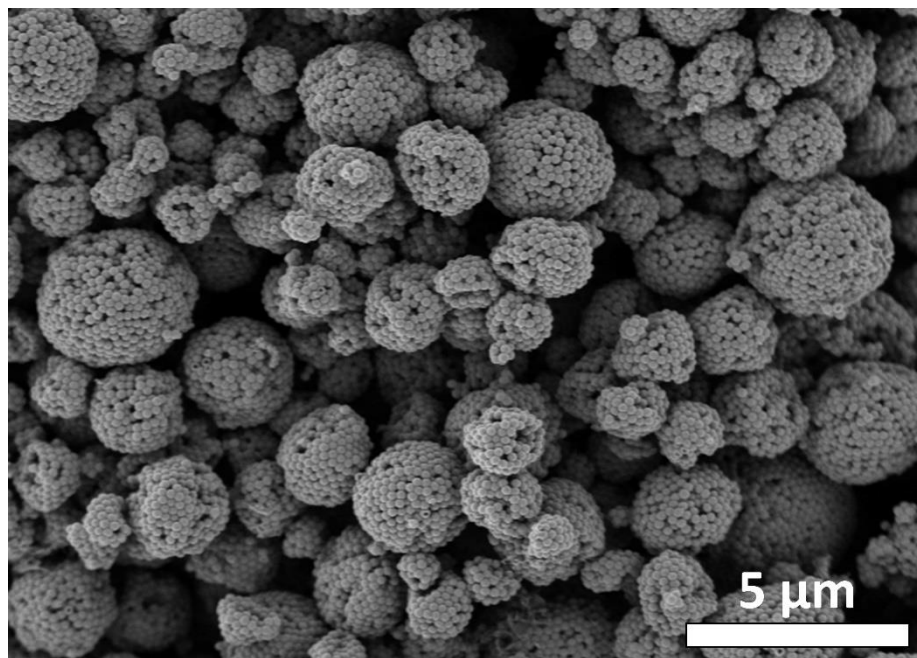


Figure S1. SEM image of HCNCs.

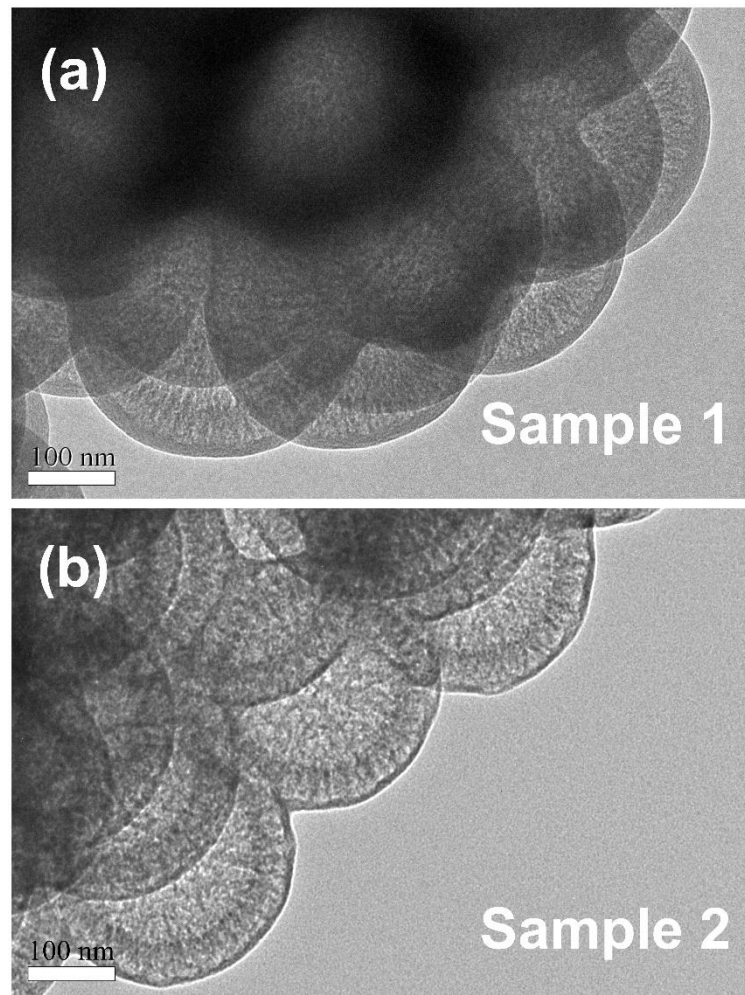


Figure S2. TEM images of HCNCs obtained with different RF precursor concentration.

Additional explanation: RF precursor concentration of sample 1 (**Fig. S2a**) is 1.5 times that of sample 2 (**Fig. S2b**).

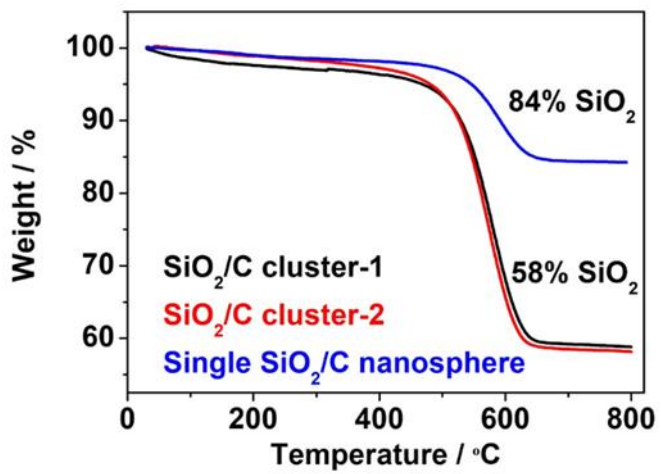


Figure S3. TGA curves of pomegranate-like SiO₂/C clusters and single SiO₂/C nanosphere under air atmosphere.

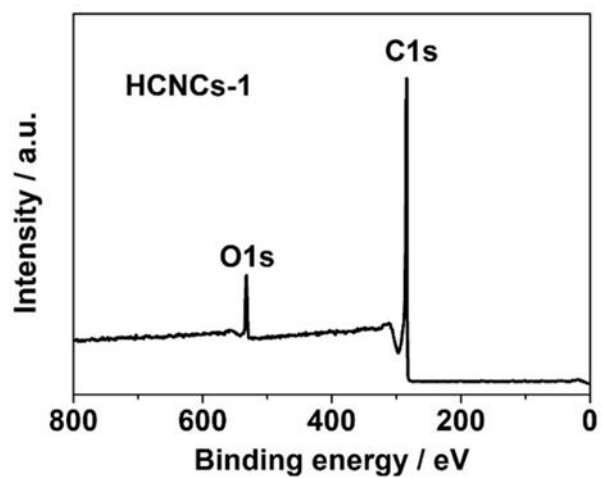


Figure S4. X-ray photoelectron spectroscopy (XPS) analysis of HCNCs-1.

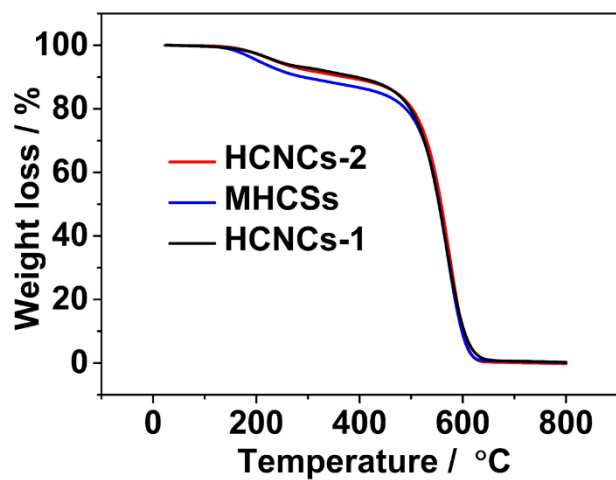


Figure S5. TGA curves of MHCSS and HCNCs under air atmosphere.

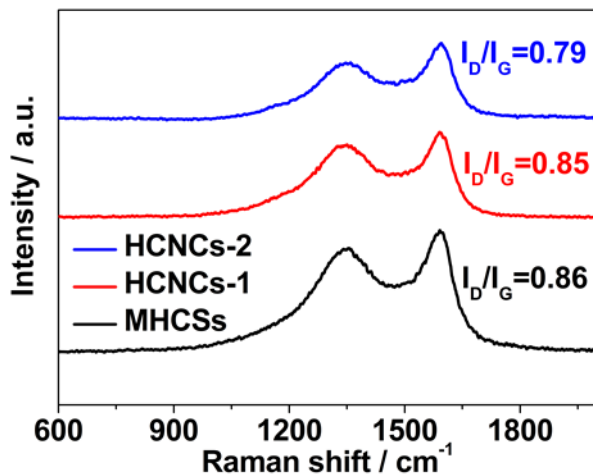


Figure S6. Raman spectra of HCNCs and MHCSSs.

Additional discussion: Only two characteristic carbon peaks at 1350 cm⁻¹ (D-band) and 1580 cm⁻¹ (G-band) are observed, which are generally related to structural defects and graphitic structure, respectively []. The intensity ratio of the D-band to G-band I_D/I_G of HCNCs-2 is 0.79, indicating the lower graphitization degree. Similarly, HCNCs-1 and MHCSSs show an amorphous carbon structure.

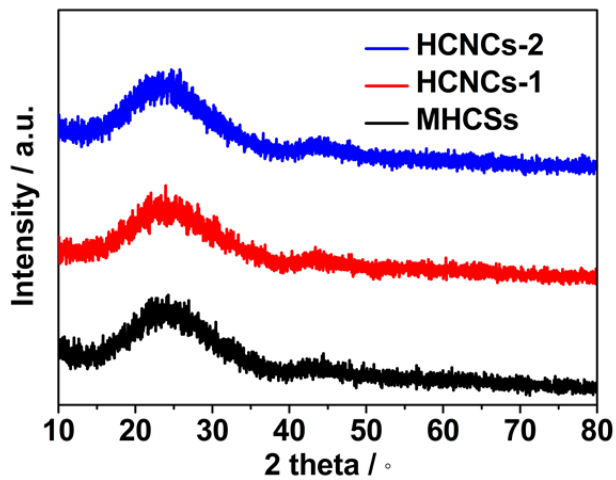


Figure S7. XRD patterns of MHCSS and HCNCs.

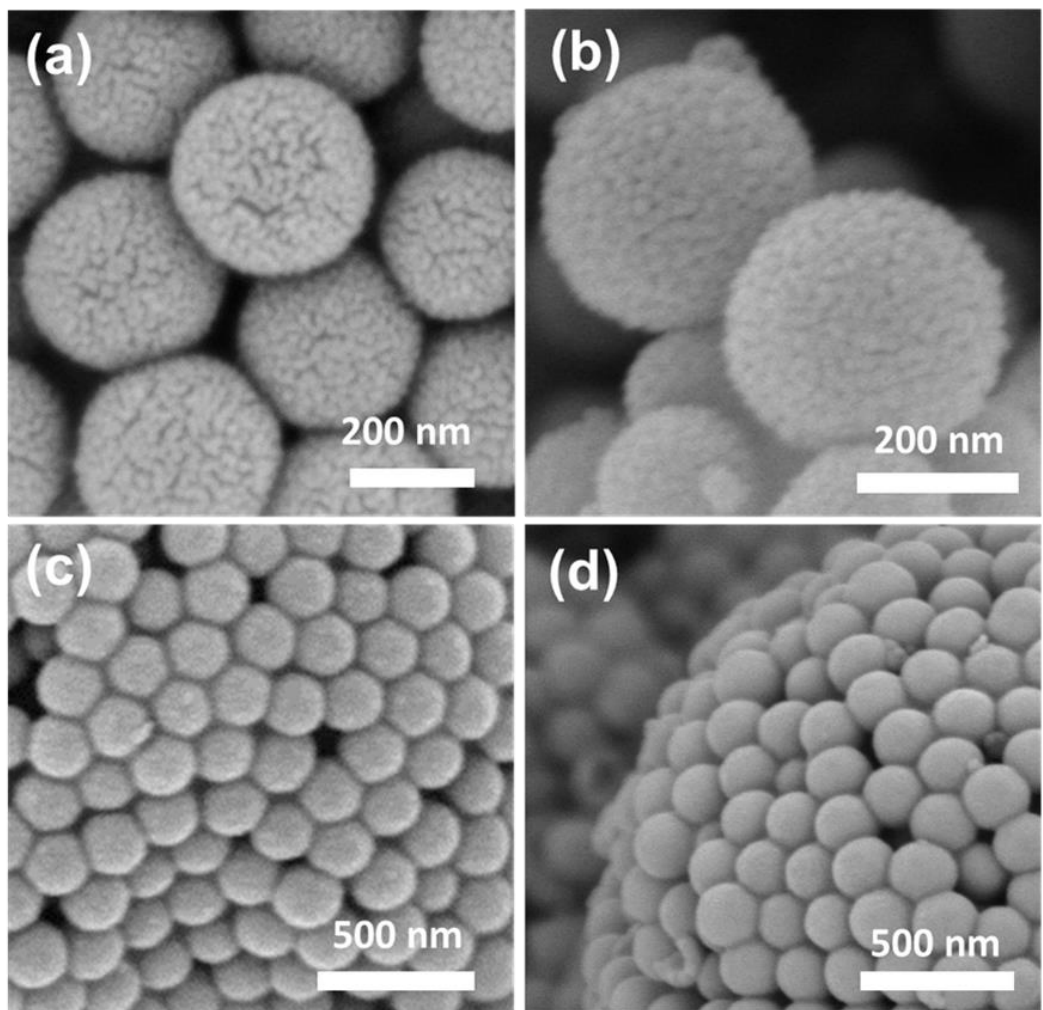


Figure S8. (a-d) SEM images of MHCSs, MHCSs/S, HCNCs-1 and HCNCs-1/S, respectively.

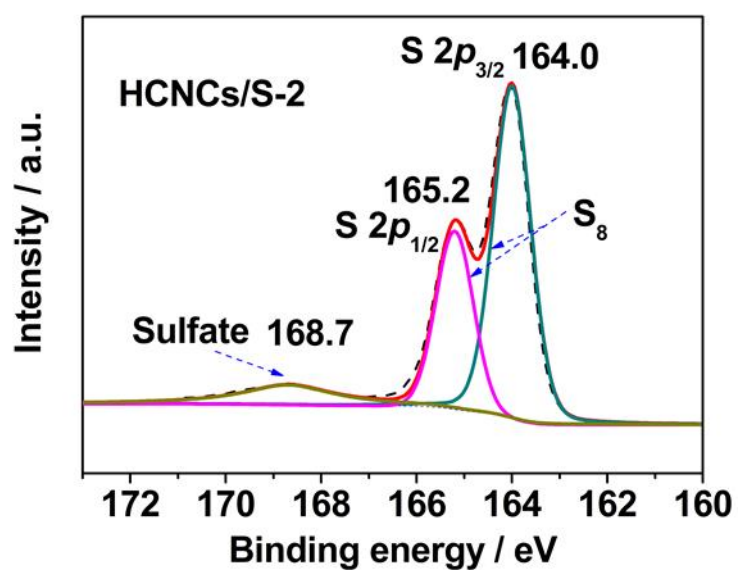


Figure S9. High-resolution S 2p spectra of HCNCs-2/S.

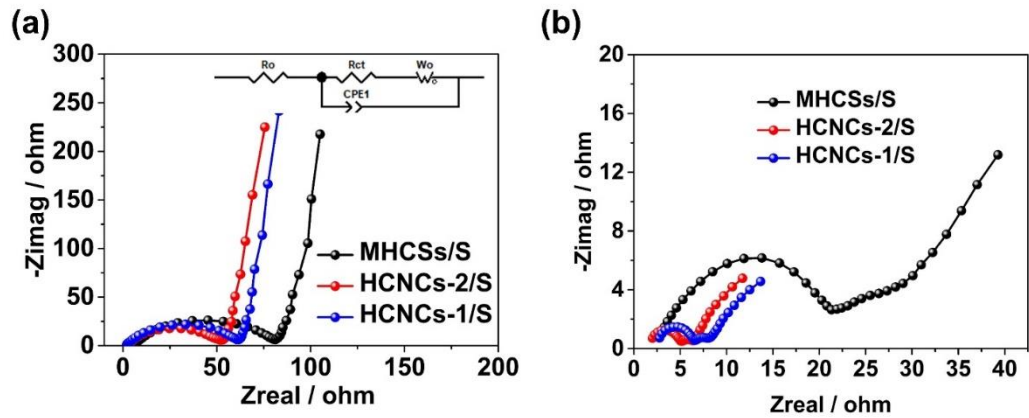


Figure S10. Nyquist plots of MHCSS/S and HCNCs/S electrode (a)before cycling and (b)after 100 cycles at 0.5 C rate.

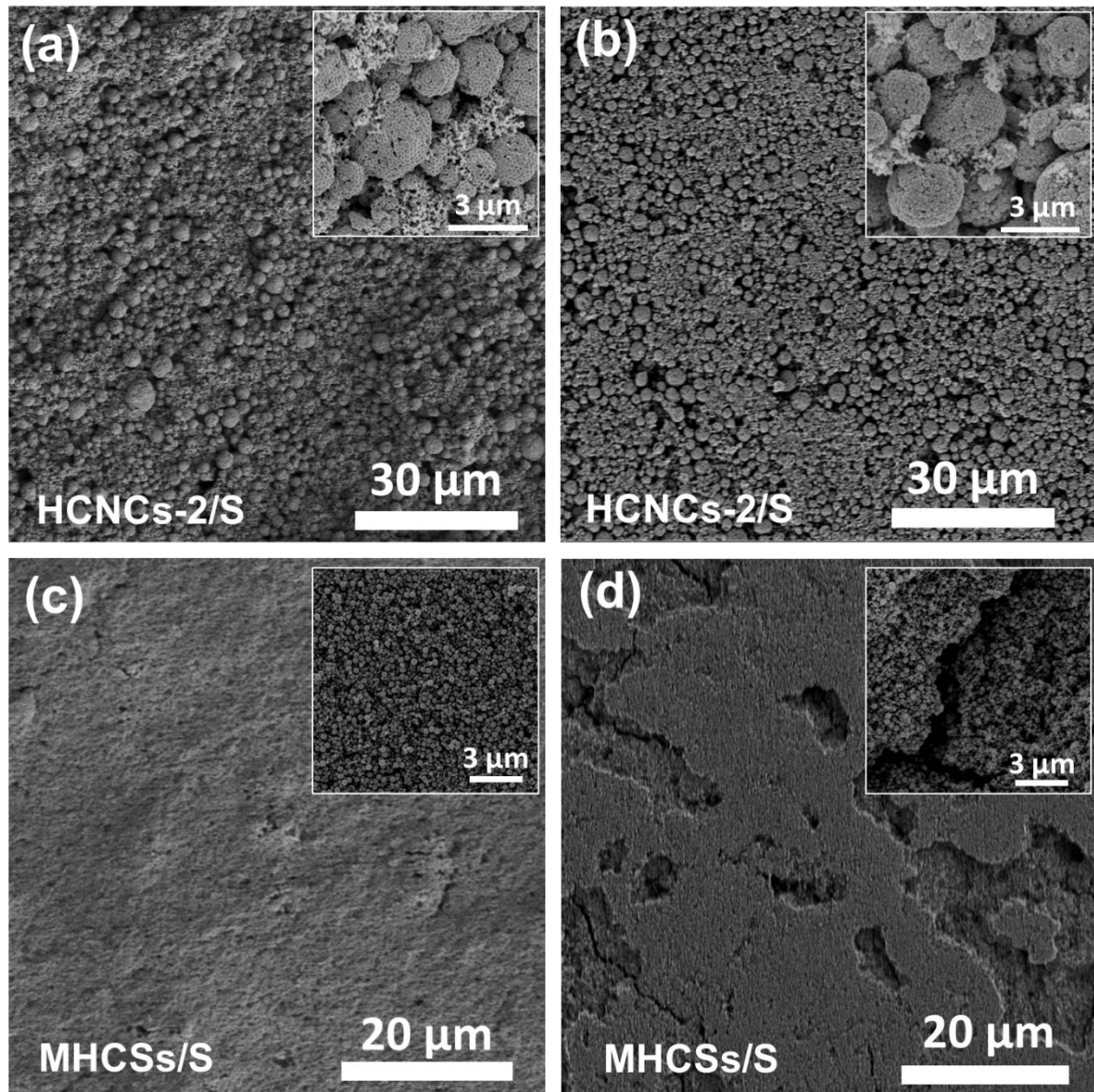


Figure S11. SEM image of the fresh (a, c) and cycled (b, d) electrodes in a charge state after 200 cycles at 1 C. Insets of (a-d) are corresponding local magnification SEM images.

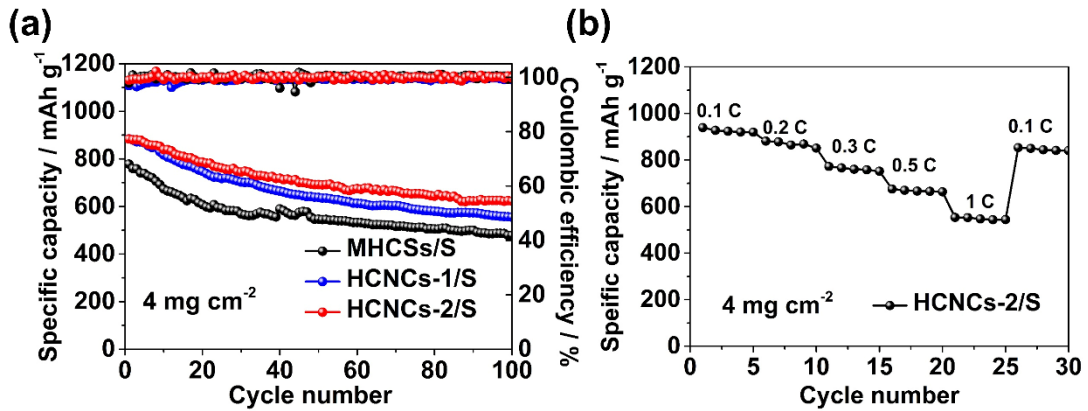


Figure S12. (a) Cycle performance of HCNCs/S and MHCSS/S electrodes with a high-sulfur-loading of 4 mg cm⁻² at 0.2 C. (b) Rate performance of HCNCs-2/S electrode with a high-sulfur-loading of 4 mg cm⁻² at varied current rates.

Table S1. XPS results of MHCSs/S and HCNCs/S.

Sample	S at.%	C at.%	O at.%
MHCSs	36.11	56.27	7.62
HCNCs-1	23.77	69.41	6.82
HCNCs-2	14.71	78.75	6.54

Table S2. Elemental analysis of MHCSs/S and HCNCs/S.

Samples	C wt.%	H wt.%	O wt.%
HCNCs-1	90.79	2.60	6.61
HCNCs-2	90.40	2.27	7.33
MHCSs	91.58	1.92	6.50

Table S3. Electrode resistance obtained from equivalent circuit fitting of the HCNCs/S and MHCSs/S cathode.

	Samples	HCNCs-1/S	HCNCs-2/S	MHCSs/S
$R_o (\Omega)$	Fresh	1.4	2.4	4.5
	After cycling	2.3	1.4	2.5
$R_{ct} (\Omega)$	Fresh	62.4	47.9	80.7
	After cycling	4.1	3.9	18.0

Table S4. Electrochemical performances comparison of HCNCs/S with the reported hollow carbon/sulfur cathodes.

	Sulfur content (wt%)	C-rate	Cycle number	Initial capacity (mA h g ⁻¹)	Reversible capacity (mA h g ⁻¹)	Capacity decay rate per cycle	High-rate capability (mA h g ⁻¹)	Ref.
HCNCs	73%	0.2 C	500	1311	695	0.094%	715 (2 C)	This work
		1 C	300	1196	630	0.158%	592 (5 C)	
PHC/S	69.75%	0.5 C	100	1071	947	0.116%	450 (3 C)	[1]
P-AB@S	66%	0.06 C	500	1221	577	0.106%	521 (0.6 C)	[2]
S@rGO-HCS	65%	0.5 C	400	901	712	0.052%	770 (4 C)	[3]
DHCSs/S	64%	0.1 C	100	-	690	-	350 (1 C)	[4]
G-NDHCS-S	62%	0.2 C	100	1360	940	0.309%	800 (1 C)	[5]
		0.5 C	200	-	520	0.19%	600 (2 C)	
S/HCSF@C	70.7%	0.6 C	300	-	780	0.14%	535 (1.2 C)	[6]
S/HICS-75	75%	0.5 C	800	933	441	0.066%	480 (1 C)	[7]
HG/S	90%	1 C	600	-	-	0.08%	676 (2 C)	[8]
		0.5 C	200	1109	910	0.03%		
HCS-S	57%	0.12 C	100	1098	844	0.23%	-	[9]
HCSs/S-LBL	65%	0.6 C	200	850	575	0.162%	698 (2.4 C)	[10]
m-DSHCS/S (containing N)	75%	0.2 C	200	1289	876	0.16%	900 (1 C)	[11]
		1 C	1000	~1090	386	0.07%	800 (2 C)	

Reference

- [1] N. Jayaprakash, J. Shen, S. S. Moganty, et al., *Angew. Chem., Int. Ed.*, 2011, 50,5904-5908.
- [2] L. X. Miao, W. K. Wang, A. B. Wang, et al., *J. Mater. Chem. A*, 2013, 1, 11659-11664.
- [3] S.K. Liu S, K. Xie, Z.X. Chen, et al., *J. Mater. Chem. A*, 2015, 3, 11395-11402.
- [4] C. Zhang, H. B. Wu, C. Yuan, Z. Guo, X. W. Lou, *Angew. Chem. Int. Ed.* 2012, 51, 9592-9525.
- [5] G. M. Zhou, Y. B. Zhao, A. Manthiram, *Adv. Energy Mater.* 2015, 5, 1402263.
- [6] J. Zang, T.H. An, Y.J. Dong, X.L. Fang, M.S. Zheng, Q.F. Dong, N.F. Zheng, *Nano Res.* 8 (2015) 2663–2675.
- [7] Y. J. Zhong, S. F. Wang, Y. J. Sha, M. L. Liu, R. Cai, Z. P. Shao, *J. Mater. Chem. A.*,2016, 4, 9526-9535.
- [8] K. Zhang, Q. Zhao, Z. Tao and J. Chen, *Nano Res.* 2013, 6, 38.
- [9] J. J. Tang, J. Yang, X. Y. Zhou, *RSC Adv.*, 2013, 3,16936-16939.
- [10] F. Wu, J. Li, Y. F. Su, J. Wang, W. Yang, N. Li, L. Chen, S. L. YChen, R. J. Chen, L. Y. Bao, *Nano Lett.*, 2016, 16, 5488-5494.
- [11] Zhang, Y., Zong, X., Liang, Z., Yu, X., Gao, J., Xun, C., Wang, Y. *Electrochimica Acta* .,2018, 284, 89-97.